ISSN 1547-4771, Physics of Particles and Nuclei Letters, 2012, Vol. 9, No. 4–5, pp. 406–409. © Pleiades Publishing, Ltd., 2012.
Original Russian Text © V.V. Parkhomchuk, S.A. Rastigeev, 2012, published in Pis'ma v Zhurnal Fizika Elementarnykh Chastits i Atomnogo Yadra, 2012, No. 4–5(174–175), pp. 666–671.

MAGNETIC AND VACUUM SYSTEMS, POWER SUPPLY FOR ACCELERATORS

Ion Selection in Accelerator Mass Spectrometer at the Budker Institute of Nuclear Physics

V. V. Parkhomchuk and S. A. Rastigeev

Budker Institute of Nuclear Physics, Siberian Branch, Russian Academy of Sciences, Novosibirsk, Russia

Abstract—This article describes the special features of the acceleration mass spectrometer (AMS) created at the Institute of Nuclear Physics for the Geochronology of the Cenozoic Era Center of Collective Use; it significantly reduces the background during the process of registering cosmogenic carbon ^{14}C. The results of experiments on measuring the background and extraction of a pure beam of radiocarbon are provided.

DOI: 10.1134/S1547477112040279

INTRODUCTION

An acceleration mass spectrometer (AMS) is used for the ultrasensitive analysis of the isotope composition of carbon [1]. In a contemporary sample (plant or animal), the concentration of the radioactive isotope of carbon (weighing 14 amu) is at the level of 10^{-12} of the main isotope. When the sample dies, the concentration of radiocarbon decreases twice every 5370 years. The sensitivity of the AMS is limited by the background of interfering ions, which have passed all stages of analyzer selection. The background flux is based on ions with close weights ^{12}C, ^{13}C, ^{14}N, ^{16}O. The processes of scattering, ionization, electron capture, and the change in energy during the process of ion charge exchange in the electric field as a result of the interaction with the residual gas and the walls of the vacuum equipment reduce the possibilities of selection. For these reasons, additional opportunities for the reduction of the ion background have been introduced into the concept of the AMS created at the Budker Institute of Nuclear Physics (BINP).

1. BINP AMS

The BINP AMS is based on an electrostatic accelerator of a tandem type with a beam turn in a high-voltage terminal [2]. The movement of ions in such AMSs can be presented as follows. The analyzed ions are formed as a result of the bombardment of the surface with cesium ions. The negative ions knocked out of the sample are horizontally accelerated in the ion source to the energy of injection (25 keV) and then turn 90° in the magnetic field and get accelerated vertically upwards in the first accelerating tube towards the positive potential of the high-voltage terminal (1 MV). The ions are stripped to the charge state 3+ on the target in the vapors of magnesium; then they turn 180° due to electrostatic turn and accelerate downwards in the second accelerator tube to the ground potential. Then the ions turn 90° in the magnetic field and get registered in the time-of-flight particle detector [3]. It should be noted that the molecular ions in the charge state 3+ are less stable and immediately decompose; in addition, the atoms of nitrogen do not form negative ions.

Electrostatic accelerators of a tandem type are the basis of most existing AMSs. The simplest construction of a tandem accelerator can be presented as two consecutive acceleration tubes; the beam passes straight through the accelerator. In this project we focus our attention on the possibility of a significant reduction in the flow of background particles by using an energy filter in the high-voltage terminal (180° electrostatic turn). In this case the background from ^{14}N ions (whose weights slightly vary from ^{14}C) can be significantly suppressed by this filter since nitrogen is formed from the fragments of the molecules which split before the electrostatic turn in the process of charge exchange; i.e., it has lower energy than the ions of radiocarbon. If nitrogen ions have not been filtered after the first stage of acceleration, on the second stage of acceleration their energy can become equal to the energy of the radiocarbon ions, making their separation in electromagnetic fields nearly impossible. The background of carbon from molecular ions $^{13}CH^-$ or $^{12}CH_2$ [4] can be efficiently suppressed in a similar way. Originally, the concentration of such molecular ions knocked out of the sample surface is 8 and more orders higher than the concentration of $^{14}C^-$ ions. Another feature of our project is the application of a magnesium-vapor target for charge exchange [5]. Such a target does not disturb the vacuum outside the heated volume and reduces the possibility that the background ions will pass the stages of AMS selection.

2. ION SELECTION

Figure 1 shows the typical time-of-flight spectrum for *a* contemporary and *b* dead carbon samples. The

position of the main peak (840 channels) corresponds to the time of flight of radiocarbon ions. Carbon tissue, which is known to be produced from contemporary plants, is used as a modern sample. The origin of carbon tissue does not require any confirming references because the large concentration of radiocarbon in the spectrum shown in Fig. 1a demonstrates the fact that carbon in the tissue has a plant origin. MPG-type graphite is used as the 'dead' sample with rather low concentration of radiocarbon. The value of the ^{14}C peak is 2×10^{-3} of ^{14}C peak in the contemporary sample, corresponding to the radiocarbon age of the sample of over 50 000 years (about nine half-life periods of ^{14}C). In the contemporary sample, the peak of the radiocarbon dominates, while the influence of the background ions is negligible. In the 'dead' sample the peaks of the background ions are comparable with the ^{14}C peak, but they are well separated in the time-of-flight region.

Figure 2 shows the distribution of the particles in the plane of two time-of-flight intervals. The results in Figs. 1 and 2 correspond to the same experimental data. It should be noted that the data show the position of each ion rather than characterize the distribution of the particle density in two-dimensional space. The absence of dots which randomly fill the space in Fig. 2 evidences the reliable work of the particle detector and the absence of any accidental responses of the detector. Figure 2 shows that the time of flight of the background ion differs in both the axis of the plot, i.e., the velocity of the background ions is different from the velocity of ^{14}C. The majority of background ions have a velocity lower than ^{14}C. Assuming that the ions of different weights have the same energy at AMS output, the 1-amu difference from ^{14}C will result in the 30-channel difference in time of flight ToF 1–3. Figure 1a illustrates that the intensity of the ^{14}C peak for the 30-channel shift is about 10^{-3} of the maximum. Although the peak of radiocarbon is significantly lower for the dead sample than for the contemporary sample, in both cases the intensities of the background ions are comparable. Obviously these peaks of background ions are not radiocarbon ions of a different energy.

Figure 3a shows the time-of-flight spectrum of oxygen ions. In this case the magnetic field of the injection magnet is adjusted for the optimal transmission of ^{16}O, but the dipole corrector of the other transverse direction deflects the beam so that the intensity of the beam is reduced to the safe value for the particle detector (several kHz) at the AMS outlet. The other parameters of the AMS correspond to the optimal transmission of ^{14}C. Two peaks created by oxygen ions are observed. The peak of lower intensity corresponds to the ions that passed through the output magnet with 'correct' energy (4025 keV). This can be easily confirmed by readjusting the output magnet for the optimal transmittance of $^{16}O^{3+}$; the result is provided in Fig 3b. The main peak in Fig. 3a refers to oxygen ions

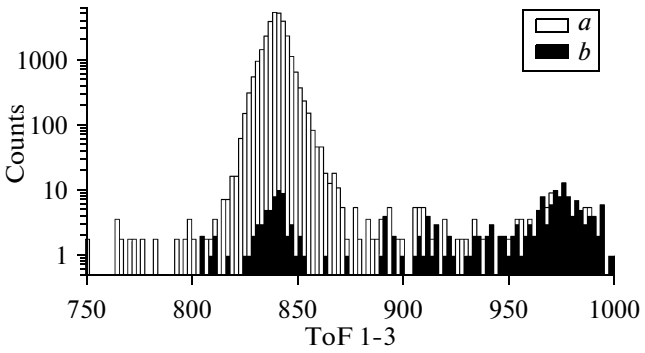

Fig. 1. Time-of-flight spectra of radiocarbon of (*a*) contemporary and (*b*) dead carbon samples. The data are normalized for the current of the stable carbon isotope.

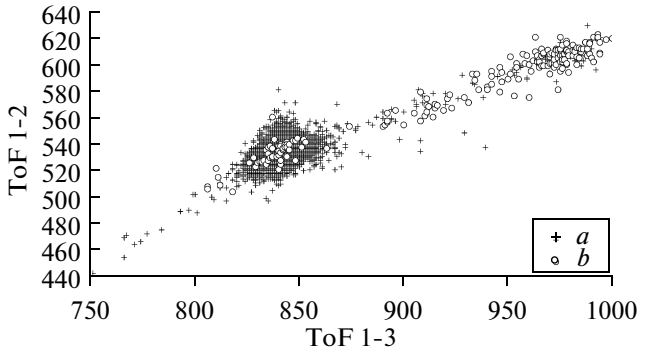

Fig. 2. Position of the ions in the two-dimensional time-of-flight space for (*a*) contemporary and (*b*) dead carbon samples.

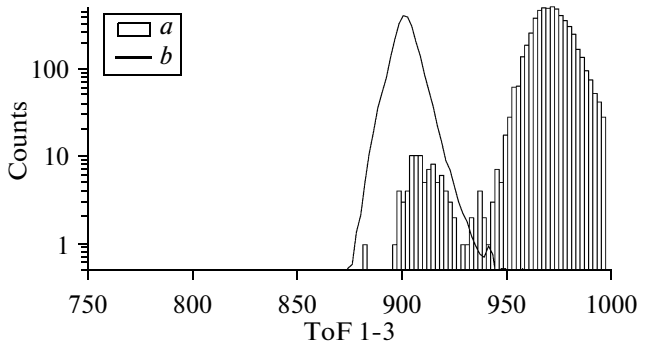

Fig. 3. Time-of-flight spectrum of the ion background of (*a*) oxygen and (*b*) the position of the peak of oxygen ions.

with reduced energy, so that their impulse corresponds to the output magnet adjusted for the optimal transmittance of $^{14}C^{3+}$. A comparison between Figs. 1 and 3a makes it possible to conclude that, in the process of radiocarbon registration, background ions with somewhat higher times of flight correspond first and foremost to oxygen ions.

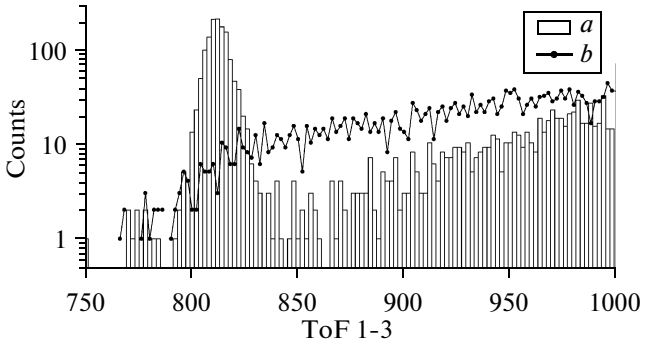

Fig. 4. Time-of-flight spectra of the ion background of the stable isotopes of carbon (*a*) ^{13}C and (*b*) ^{12}C.

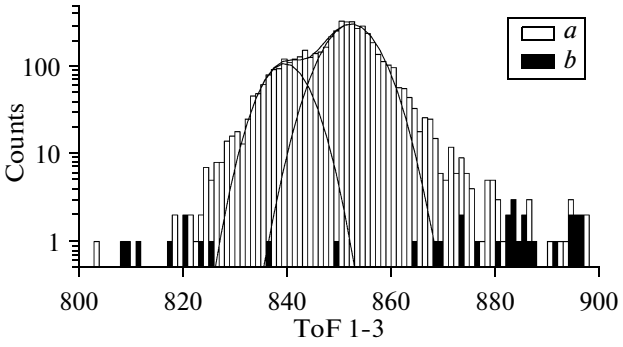

Fig. 5. Time-of-flight spectra of the ion background of nitrogen for (*a*) the working value of the field of the electrostatic filter in the high-voltage terminal and (*b*) the readjusted value for the transmission of nitrogen ions (the imitation of the absence of the filter).

Other ions that have close weights and therefore cause a noticeable ion background are the main stable isotopes of carbon ^{12}C and ^{13}C. Figure 4 shows the time-of-flight spectrum of the carbon isotopes. The adjustment of the AMS is performed similarly to the experiment shown in Fig. 3a, except for the adjustment of the injection magnet for the transmission for either ^{12}C or ^{13}C ions. Figure 4a shows the peak of ^{13}C ions with correct energy. In the radiocarbon range there is a two-order collapse and then the concentration of the background ions increases along with the decrease in energy and remains one order lower than the main peak. A comparison between Figs. 1 and 4a makes it possible to conclude that the spectrum of radiocarbon con^{t}ains a small peak of ^{13}C and the background ions of ^{13}C make only a negligible contribution in the region with a high time of flight. The spectrum of ^{12}C ions does not have obvious peaks, as is shown in Fig. 4b. This spectrum shows that the intensity of the appearance of ^{12}C ions in the radiocarbon region is somewhat lower than the intensity of the ^{12}C ions in the region of high times of flight. Since in Fig. 1 there is a collapse of intensity on the right from the peak of radiocarbon, one can assume that in the process of radiocarbon registration the contribution of ^{12}C ions to the ion background is negligible.

Nitrogen does not form stable negative ions. In order to check the possible presence of nitrogen ions at the outlet of the AMS, we have injected NH^- ions in the acceleration mode similarly to the experiment in Fig. 3a; the result is presented in Fig. 5a. Most nitrogen atoms have been filtered by the electrostatic turn in the high-voltage terminal of the accelerator since NH molecules split before the turn and after the split the nitrogen ions have 14/15 of kinetic energy of NH molecules. Such a significant difference in energy makes it possible to filter the background ions of nitrogen in the high-voltage terminal even at the outlet of the AMS with the linear construction of the tandem accelerator (without a turn after the first stage of the acceleration). However, the process of the ion exchange in the second acceleration tube can lead to the additional acceleration of the ions, thereby compensating for the lower energy of nitrogen ions after the first stage of the acceleration. If the kinetic energy of nitrogen and radiocarbon is the same at the outlet of the accelerator, it is hardly possible to separate them by movement in electromagnetic fields due to their insignificant difference in weights. The separation is possible only by the difference in the ionization losses due to the difference in the nucleus charge if the ion concentrations at the outlet of the AMS are comparable. For the low-energy ion, the reliability of the ionization loss detector is limited by the necessity of applying thin, strong, and uniform inlet windows (films) and the serious requirement for the low noise level in the applied electronics due to weak signals of the ionization losses. In the BINP AMS, the nitrogen ions are screened out before they enter the final particle detector. Figure 5b demonstrates that only nitrogen ions with the same kinetic energy as radiocarbon can enter the AMS outlet. The conditions of the experiment are identical to the experiment shown in Fig. 5a, but the turn in the high-voltage terminal is adjusted for the transmission of nitrogen ions (NH fragments) with charge 4+. Figure 5b shows the double peak. The right component of the peak corresponds to a higher time of flight compared to radiocarbon (Fig. 1) as determined by the lower energy of nitrogen obtained from the split molecules. However, the left component of the peak in Fig. 5b corresponds to the time of flight of radiocarbon ions. This peak is determined by nitrogen ions that move into the second acceleration tube with charge 4+ and then recharge for 3+. Since the kinetic energy acquired in the process of acceleration is proportional to the ion charge and the average charge exceeds 3+ (the charge of radiocarbon ions at the second stage of the acceleration), the formed nitrogen ions have the same kinetic energy as radiocarbon. Let us note that the mechanism of nitrogen ion transmission shown in Fig. 5b is just one possible mechanism. If there is no turn in the ter-

minal, ions with all possible charge states and significant energy dispersion can gel into the second acceleration tube and lead to a increase in the transmitted background of nitrogen when compared to the one presented in this figure. We should add that the time of statistical accumulation for Figs. 5a and 5b is the same. A comparison between Figs. 5a and 5b demonstrates the efficient suppression of nitrogen background with an energy filter in the high-voltage terminal.

CONCLUSIONS

The efficient suppression of the nitrogen background in the BINP AMS was demonstrated. The ion background observed in the process of radiocarbon measurement was studied. It was shows that the influence of the ion background is negligible in the measurement of radiocarbon concentration of $^{14}C/^{12}C \sim 2 \times 10^{-15}$ (MGP-type graphite).

REFERENCES

1. C. Tuniz, J. R. Bird, D. Fink, et al., *Accelerator Mass Spectrometry: Ultrasensitive Analysis for Global Science* (CRC, 1998), p, 18.
2. N. I. Alinovskii, A. D. Goncharov, V. F. Klyuev, et al., Tech. Phys. **54**, 1350 (2009).
3. N. I. Alinovskii, E. S. Konstantinov, V. V. Parkhomchuk, et al., Instrum. Exp. Tech. **52**, 234 (2009).
4. V. V. Parkhomchuk and S. A. Rastigeev, Tech. Phys. **54**, 1529 (2009).
5. V. F. Klyuev, V. V. Parkhomchuk, and S. A. Rastigeev, Instrum. Exp. Tech. **52**, 245 (2009).